

No-Reference Image Quality Assessment via Feature Fusion and Multi-Task Learning

S. Alireza Golestaneh
Robotics Institute
Carnegie Mellon University
Pittsburgh, USA

Kris Kitani
Robotics Institute
Carnegie Mellon University
Pittsburgh, USA

ABSTRACT

Blind or no-reference image quality assessment (NR-IQA) is a fundamental, unsolved, and yet challenging problem due to the unavailability of a reference image. It is vital to the streaming and social media industries that impact billions of viewers daily. Although previous NR-IQA methods leveraged different feature extraction approaches, the performance bottleneck still exists. In this paper, we propose a simple and yet effective general-purpose no-reference (NR) image quality assessment (IQA) framework based on multi-task learning. Our model employs distortion types as well as subjective human scores to predict image quality. We propose a feature fusion method to utilize distortion information to improve the quality score estimation task. In our experiments, we demonstrate that by utilizing multi-task learning and our proposed feature fusion method, our model yields better performance for the NR-IQA task. To demonstrate the effectiveness of our approach, we test our approach on seven standard datasets and show that we achieve state-of-the-art results on various datasets.

CCS CONCEPTS

• **Computing methodologies** → **Image processing**; *Computer vision*; *Image and video acquisition*; *Image compression*.

KEYWORDS

No-reference image quality assessment, multi-task learning, natural images, screen content images, and HDR-processed images.

1 INTRODUCTION

Image and video compression and applications of visual media continue to be in high demand these days. There has been an increasing demand for accurate image and video quality assessment algorithms for different multimedia and computer vision applications, such as image/video compression, communication, printing, display, restoration, segmentation, and fusion [7, 16, 37, 74]. Robustness of different multimedia and computer vision applications heavily relies on their input's quality. Therefore, it is of great importance to be able to automatically evaluate image quality in the same way as it perceived by the human visual system (HVS). Furthermore, in many real-world applications, IQA task needs to be carried out in a timely fashion on a computationally limited platform.

Objective quality metrics can be divided into full-reference (reference available or FR), reduced-reference (RR), and no-reference (reference not available or NR) methods based on the availability of a reference image [61]. FR methods [24, 52, 53, 77] usually provide the most precise evaluation results and perform well in predicting the quality scores of human subjects in comparison with RR and NR

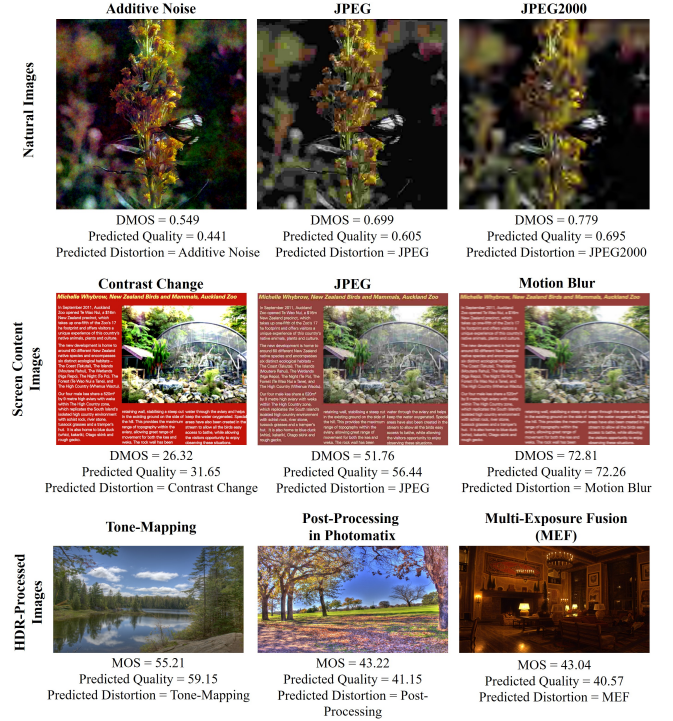


Figure 1: Example results of our proposed NR-IQA method. First, second, and third rows show images with different distortion types (distortion type is provided on the top of each image) taken from datasets with natural images, screen content images, and HDR-processed images, respectively. MOS and DMOS represent the subjective image quality scores; as DMOS (MOS) increases (decreases) the quality of the image degrades more. Under each image we provide the predicted distortion type as well as quality score computed via our proposed method.

methods. RR methods [11, 55] provide a solution when the reference image is not fully accessible. These methods generally operate by extracting a minimal set of parameters from the reference image; these parameters are later used with the distorted image to estimate quality. However, in many practical applications, an IQA system does not have access to reference images. Without the reference image, IQA task becomes very challenging. The goal of the no-reference image quality assessment (NR-IQA) methods [2, 9, 10, 13–15, 18, 19, 21–23, 25, 26, 33–36, 38–44, 51, 57–60, 63–68, 70–73, 75, 76, 78] is to provide a solution when the reference image is not available.

NR-IQA methods are mainly divided into two groups, distortion-based and general-purpose methods. A distortion-based approach is to design NR algorithms for a specific type of distortion (e.g. blocking, blurring, or contrast distortions). Distortion-based approaches have limited applications in more diverse scenarios. A general-purpose approach is designed to evaluate image quality without being limited to distortion types. General-Purpose methods usually make use of extracted features that are informative for various types of distortions. Therefore, performance highly depends on designing elaborate features. Existing general-purpose NR-IQA methods can mainly be classified into two categories depending on the types of features used.

The first category is based on well-chosen handcrafted features that are sensitive to the image quality (e.g. natural scene statistics, or image gradients). Natural scene statistics (NSS) [43, 52] is one of the most widely used features for IQA. NSS has the assumption that natural images have statistical regularity that is altered when distortions are introduced. Various types of NSS features have been defined in transformation domain [51, 51, 67], and spatial domain [33, 41, 42, 75]. The main constraint of NSS is its limitation in capturing and modeling the deviation among different similar distortions. Moreover, the limitation of using handcrafted features is the lack of generalizability for modeling the multiple complex distortion types or contents. As we will show in the results section, methods based on handcrafted features that are designed for natural images will not perform well for screen content images (SCIs) or high-dynamic-range- (HDR) processed images.

The second category is based on utilizing feature learning methods. Inspired by the performance of convolutional neural networks (CNNs) for different computer vision applications, different works utilize them for NR-IQA task. The key factor behind achieving good performance via deep neural networks (DNNs) is having massive labeled datasets [6] that can support the learning process [28]. However, existing IQA datasets contain an extremely low number of labeled images. Moreover, unlike generating datasets for image recognition task, generating large-scale reliable human subjective labels for quality assessment is very difficult. Obtaining an IQA dataset requires a complex and time consuming psychometric experiment. Furthermore, applying different data augmentation methods to increase the number of data can affect perceptual quality scores. Nonetheless, different approaches such as transfer learning, generative adversarial networks (GANs), and proxy quality scores have been used to leverage the power of DNNs for NR-IQA. Many researchers achieved state-of-the-art results by using DNNs for NR-IQA task. With the exception of just a few number of algorithms [19, 23, 39, 60, 65, 66], existing NR-IQA methods heavily rely only on the subjective quality scores to predict the quality. Most of the learning-based methods ignore how utilizing distortion during training can be beneficial to predict the perceptual quality, similar to the way that HVS perceives the quality.

It is common to use multiple sources of information jointly in human learning. Babies learn a new language by listening, speaking, and writing it. The problem of using a single network to solve multiple tasks has been repeatedly pursued in the context of deep learning for computer vision. Multi-task learning has achieved great performance for a variety of vision tasks, such as surface normal and depth prediction [8, 49], object detection [45], and navigation [79].

The perceptual process of the HVS includes multiple complex processes. The visual sensitivity of the HVS varies according to different factors, such as distortion type, scene context, and spatial frequency of stimuli [5, 32, 62]. The HVS perceives image quality differently among various image contents [1, 4]. Image quality assessment and distortion identification tasks are closely related. During the feature learning process, identifying the distortion not only helps the image quality assessment task, but also can open up the opportunity to enhance the quality of the distorted image based on the degradation type. By leveraging the distortion type for the IQA task, our model predicts the distortion type as well as the quality score of a distorted image during testing. Fig 1 shows example results of our proposed method.

From a modeling perspective, we are interested in answering: How does the additional distortion information influence NR-IQA and how much does it improve the overall performance? What is the best architecture for taking advantage of distortion information for NR-IQA? We examine these questions empirically by evaluating multiple DNN architectures that each take a different approach to combine information. Our proposed method improves upon the following limitations of recent works on multi-task learning for NR-IQA [19, 23, 39, 60, 65, 66]. 1) The general trend among the recent multi-task NR-IQA methods [19, 23, 39, 60, 65] are to use overparameterized sub-networks or fully connected layers (FCL) for different tasks to achieve higher performance. In many real-world applications (e.g. self-driving cars and VR/AR) IQA task needs to be carried out in a timely fashion on a computationally limited platform. We propose a pooling and fusion method along with 1×1 convolution layer which replace the overparameterized FCL for each task. 2) Except for few methods, multi-task NR-IQA methods [65, 66] use multi-stage training and optimize each task separately to achieve the best performance. In contrast, our method is simply trained end-to-end in one step without any multi-stage training. 3) Existing approaches without providing any analysis used the last layer of the network for all the tasks. They further use sub-networks or FCL for each task and rely on overparameterized learning layers to achieve good performance. In this work, we empirically investigate the effect of feature fusion for NR-IQA task. Using our design and feature fusion, we show that by using only 1×1 convolution layers along with global average pooling (GAP) we can achieve a better performance. From a computational perspective, by using a smaller backbone in our experiments compared to existing models, our proposed model outperforms many of the existing state-of-the-art single-task and multi-task IQA algorithms.

We propose an end-to-end multi-task model, namely *QualNet*, for NR-IQA. During the training stage, our model makes use of distortion types as well as subjective human scores to predict the image quality. We evaluate our approach against different NR-IQA methods and achieve state-of-the-art results on several standard IQA datasets. We provide extensive experiments to demonstrate the effectiveness of our proposed method and architecture design.

In summary, our contributions are summarized as follows:

- We propose an end-to-end multi-task learning approach for blind quality assessment and distortion prediction. We propose a feature fusion method to utilize distortion information for improving the quality score estimation task. Specifically,

given an input image, our proposed model is designed to regress the quality and predict the distortion type (or distortion types).

- We provide empirical experiments and evaluate different feature fusion choices to demonstrate the effectiveness of our proposed model.
- We evaluate the performance of our proposed method on three well-known natural image datasets (LIVE, CSIQ, TID2013). While using a smaller backbone for feature extraction, our model outperforms the existing algorithms on two datasets (CSIQ and TID2013). We also test the performance of our method on the LIVE multi-distortion dataset and outperform the state-of-the-art NR-IQA methods. In addition to natural image datasets, we further evaluate the performance of our algorithm on two other datasets with different scene domains (screen content images and HDR-processed images) and achieve state-of-the-art results.

2 RELATED WORK

We briefly review the literature related to our approach.

2.1 Single-Task NR-IQAs

Before the rise of deep neural networks (DNNs), NR-IQA methods utilize different machine learning techniques (e.g. dictionary learning) or image characteristics (e.g. NSS) to extract the features for predicting the quality score. CORNIA [71] used a dictionary learning method to encode the raw image patches to features. CORNIA features later were adopted in some NR-IQA models [38, 70, 76].

With the progress of DNNs in different applications, more researchers have utilized them for NR-IQA. In [22] the authors proposed a shallow CNN for feature learning and quality regression. [26] developed a two-stage model that separated into an objective training stage followed by a subjective training stage. In the first stage, they used PSNR to produce proxy scores. Then, they generated the feature maps which were then regressed onto objective error maps. The second stage aggregated the feature maps by weighted averaging and finally regressed these global features onto ground-truth subjective scores. [44] proposed a deep learning based model (BP-SQM) which consists of a fully convolutional neural network and a deep pooling network. Given a similarity index map, labels generated via a FR-IQA model, their model produced a quality map that model the similarity index in pixel distortion level. Hallucinated-IQA [35] proposed a NR-IQA method based on generative adversarial models. They first generated a hallucinated reference image to compensate for the absence of the true reference. Then, paired the information of hallucinated reference with the distorted image to estimate the quality score. Although [26, 35, 44] perform well for the NR-IQA task, they all used some sort of the reference image during their training which contradicts the NR-IQA purpose.

2.2 Multi-Task NR-IQAs

There are a few algorithms that attempt to do NR-IQA by leveraging the power of multi-task learning. [23, 60, 65] designed a multi-task CNN to predict the type of distortions and image quality from the last fully connected layer in the network. [66] developed a multi-task rank-learning-based IQA (MRLIQ) method. They constructed

multiple IQA models, each of which is responsible for one distortion type. [39] proposed MEON, which is a multi-task network where two sub-networks train in two stages for distortion identification and quality prediction. [19] proposed a model that used multi-task learning and dictionary learning for NR-IQA.

Among the aforementioned algorithms, [65, 66] do not train end-to-end and requires multi-stage training. Although [39] is an end-to-end method, the training process is performed in two steps. Existing methods mostly used just one fully connected layer for both tasks. To the best of our knowledge, none of the existing works investigate the effect of feature fusion for NR-IQA task. In this work, we investigate different feature fusion architectures to improve the performance of NR-IQA. While taking advantage of multi-task learning, we use feature fusion from different blocks of the network to estimate the quality score more accurately. Unlike the existing multi-task NR-IQA methods, we use global average pooling instead of fully connected layers which reduces learning parameters. We observe that using fully connected layers can cause overfitting and the network memorizes the training examples rather than generalizing from them.

3 OUR APPROACH

In this section, we introduce our proposed multi-task model, *QualNet*, for NR-IQA. *QualNet* jointly learns distortion prediction as well as quality score prediction tasks. Our proposed model is fully convolutional and is trained in an end-to-end manner. An overview of the *QualNet* architecture is given in Fig. 2.

3.1 Problem Formulation

Given a distorted image I_d , our goal is to estimate its distortion type (or distortion types) as well as quality score. We partition the distorted image into overlapped patches I_k . Let f_ϕ represents proposed network with learnable parameters ϕ . Given an input image we have:

$$\mathbf{d}, s = f_\phi(I_k) \quad (1)$$

where I_k is the input image to our network, and s denotes the regressed quality score. \mathbf{d} is a $m \times 1$ vector, where m indicates the total number of distortion types available in dataset. The element of \mathbf{d} with maximum value represents the index for the distortion type.

3.2 Network architecture

QualNet is not limited by the choice of network architecture, any of state-of-the-art DNNs [17, 54, 56] can be used as a backbone for our proposed method. However, in order to emphasize the advantage of our method, we choose VGG16 which is a relatively smaller network compared to VGG19, Resnet34, or Resnet50, which are the ones that mostly used in the recent proposed NR-IQA methods [19, 35, 44, 64]. Choosing a large network easily increases the number of parameters and makes the network prone to overfitting instead of learning a better representation.

We show the architecture of our proposed model in Fig. 2. We modified VGG16 network to be used as the backbone. We add instant normalization (IN) layer after each convolution layer. However, in order to not increase the number of learnable parameters we set the trainable parameters for IN layers to be False. Despite most of the existing deep learning based NR-IQA methods that use fully connected layers (FCL) for regressing the quality score, we did not

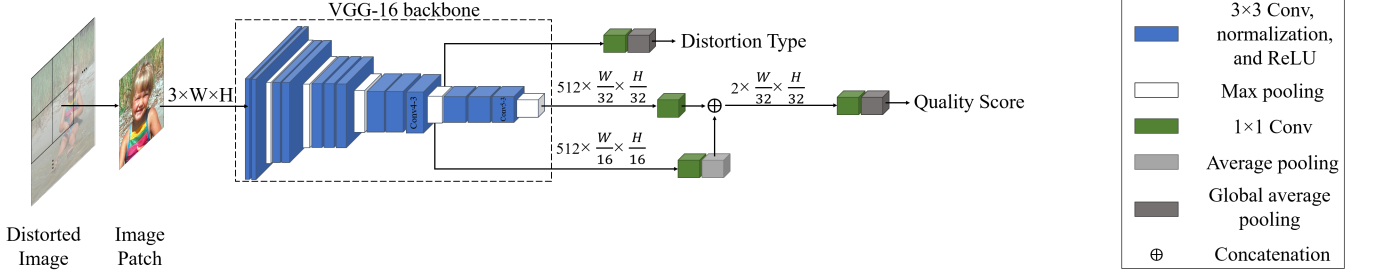


Figure 2: Architecture of our proposed multi-task learning model. Conv indicates the convolutional layers, and normalization indicates instant normalization layers.

use any fully connected layer in the head of our network, instead, we use global average pooling (GAP). The use of GAP allows networks to function with less computational power and have better generalization performance. In the head of our network, we use 1×1 convolution layer along with GAP layer for each task.

The insight behind our network design comes from two observations. **a)** Typically, different FCL/sub-networks is used at the last layer of the backbone to separately compute each task. We empirically observe that selecting features from the same layer of the network can reduce the learning capability of that layer for both of the tasks. That explains why previous models needed additional overparameterized FCL/subnetwork in their architectures. Therefore, here we choose features from different layers for each task. **b)** Inspired by the work done in the field of understanding human visual perception and psychology, we know that human vision has different sensitivities to different levels and types of distortions [5, 32, 62]. Thus, for quality score prediction task it is important to take advantage of the features used to predict the type of distortion. Fusion among features for tasks that are related can significantly capture the relative information and improve the performance by considering the relative information among all the different tasks. We proposed to fuse the features used for distortion prediction task with the quality prediction features. Using our proposed feature fusion, our method can perform efficiently and effectively well on different datasets without having overparameterized layers for each task.

3.3 Distortion Prediction

We use features of the max-pooling layer after *conv4_3* layer for the distortion prediction task. The output of max-pooling layer has $512 \times \frac{W}{16} \times \frac{H}{16}$ dimension; 1×1 convolution along with GAP is used to compute the distortion type. The output of 1×1 convolution has $m \times \frac{W}{16} \times \frac{H}{16}$ dimension, where m is the total number of distortions available in the training data. GAP layer is used to convert the $m \times \frac{W}{16} \times \frac{H}{16}$ feature map to $m \times 1$ vector, which denotes by \mathbf{d} . In the case of single distortion type, the element of \mathbf{d} with maximum value represents the index for the distortion type.

3.4 Quality Score Regression

We use features of the max-pooling layer after *conv4_3* and *conv5_3* for the quality score regression task. We first regress *conv4_3* and *conv5_3* features separately to obtain two coarse quality score maps. The average pooling layer is used to make sure that the output of 1×1

convolutions after *conv4_3* has the same dimension (i.e. $1 \times \frac{W}{32} \times \frac{H}{32}$) with the output of 1×1 convolutions after *conv5_3*. Finally, we combine the computed quality score maps by concatenating them and send it to a 1×1 convolution and GAP to achieve the final quality score.

The HVS perceive image quality differently based on different distortion types; by concatenating the features from the layer that is used to predict the distortion type we observe that our model can utilize distortion type information for quality score prediction. As shown in our ablation study, using our proposed feature fusion, we achieve the best performance.

3.5 Training

Here we describe the training details of the *QualNet*. Given \mathbf{d} and s as the output of our model, we use negative log-likelihood loss (which is simply a cross-entropy loss) and L2 loss for optimizing distortion prediction and quality score regression tasks, respectively. In other words, the total loss for our network is defined as:

$$L_{total} = L_d + \lambda L_s \quad (2a)$$

$$L_d(\mathbf{d}, c) = -\log\left(\frac{\exp(d_c)}{\sum_{j=1}^m \exp(d_j)}\right) \quad (2b)$$

$$L_s = |s - g_d|^2 \quad (2c)$$

where L_d and L_s are the losses for distortion type prediction and quality score regression, respectively. λ is a regularization parameter that in our network is set to 1. Eq. (2b) is the criterion that combines softmax and negative log-likelihood loss to train the distortion type classification problem with m classes. In other words, m is the number of distortion types. c denotes class index in the range $[1, m]$ as the target for the input. \mathbf{d} is a $1 \times m$ vector which represents the output of the distortion type prediction task. In Eq. (2c), s and g_d are regressed quality score and subjective human score for the image I_d , respectively.

In *QualNet* framework, the sizes of input images must be fixed to train the model on a GPU. Therefore, each input image should be divided into multiple patches of the same size. In our experiment, we choose patch size of 128×128 , we set the step of the sliding window to 64, i.e. the neighboring patches are overlapped by 64 pixels. We consider the patch size large enough to reflect the overall image quality, we set the quality score of each patch to its distorted images subjective ground-truth score. The effect of different patch

sizes is provided in our ablation study. To expand the training data set, the horizontal flip is performed in our training process for data augmentation.

For both tasks, our network is optimized end-to-end simultaneously. The proposed network is trained iteratively via backpropagation over a number of 50 epochs. We set batch size to 1. For optimization, we use the adaptive moment estimation optimizer (ADAM) [27] with $\beta_1 = 0.9$, $\beta_2 = 0.999$, we set the initially learning rate to 2×10^{-4} . We set the learning rate decay to 0.98, and it applied after every 3 epochs. We fine-tune our model end-to-end while using pretrained Imagenet weights to initialize the weights of the VGG16 network, the rest of the weights in the network are randomly initialized. Similar to the existing NR-IQA models for all of our evaluations, to train and test the *QualNet*, we randomly divide the reference images into two subsets, 80% for training and 20% for testing. Then, the corresponding distorted images are divided into training and testing sets so that there are no overlaps between the two. All the experiments are under ten times random train-test splitting operation, and the median SROCC and LCC values are reported as final statistics.

4 RESULTS

In this section, the performance of our proposed model is analyzed in terms of its ability to predict subjective ratings of image quality as well as distortion type. We evaluate the performance of our proposed model extensively. We use seven standard image quality datasets for our performance evaluation. For a distorted image I_d , the final predicted quality score is simply defined by averaging the predicted quality scores over all the patches from I_d . Also, the final image distortion is decided by a majority voting of the patches belong to I_d , i.e. the most frequently occurring distortion on patches determines the distortion of the image.

First, we study the effectiveness of our proposed model in regards to its ability to predict the image quality in a manner that agrees with subjective perception. For performance evaluation, we employ two commonly used performance metrics. We measure the prediction monotonicity of *QualNet* via the Spearman rank-order correlation coefficient (SROCC). This metric operates only on the rank of the data points and ignores the relative distance between data points. We also apply regression analysis to provide a nonlinear mapping between the objective scores and either the subjective mean opinion scores (MOS) or difference of mean opinion scores (DMOS). We measure the Pearson linear correlation coefficient (LCC) between MOS (DMOS) and the objective scores after nonlinear regression.

We further provide accuracy of *QualNet* for the distortion type prediction task. Finally, we provide ablation studies to evaluate the performance of *QualNet* for different choices of architecture, fusion, patch sizes, and optimization strategy.

4.1 Datasets

The detailed information for datasets that we use for our evaluation is summarized in Table 1. Specifically, we perform experiments on seven widely used benchmark datasets. For natural images use LIVE [53], CSIQ [31], TID2008 [47], TID2013 [46], LIVE-MD [20]. For SCIs we use SIQAD [69], and for images with different

tone-mapping, multi-exposure fusion, and post-processing we use ESPL-LIVE HDR [29].

Table 1: Summary of the datasets evaluated in our experiments.

Databases	# of Dist. Images	# of Dist. Types	Multiple Distortions per images?	Score Type
LIVE	799	5	NO	DMOS
CSIQ	866	6	NO	DMOS
TID2008	1700	17	NO	MOS
TID2013	3000	24	NO	MOS
LIVE-MD1	255	2	YES	DMOS
LIVE-MD2	255	2	YES	DMOS
SIQAD	980	7	NO	DMOS
ESPL-LIVE HDR	1811	11	NO	MOS

4.2 Natural Images

Most of the existing NR-IQA designed to predict the quality of natural images. Table 2 shows the obtained performance evaluation results of our proposed algorithm on the LIVE, CSIQ, TID2013, LIVE-MD1, and LIVE-MD2 datasets in comparison with state-of-the-art general-purpose NR-IQA algorithms. As shown in Table 2, our proposed method outperforms state-of-the-art algorithms on several datasets while having a smaller backbone. We believe that this improvement is because of our feature fusing and taking advantage of multi-task learning. Although [35] achieved the best performance for SROCC on LIVE dataset, it has bigger backbone compared to us (VGG19 vs VGG16). Moreover, as shown in Table 2, our proposed model achieves the highest performance when we average the performances among all the datasets.

Cross-dataset evaluations. To evaluate the generalizability of the *QualNet*, we conduct cross dataset test. Training is performed on LIVE, and then the obtained model is tested on TID2008 (for comparability) without parameter adaptation. Both quality score regression and distortion type prediction tasks are tested. We follow the common experiment setting to test the results on the subsets of TID2008, where four distortion types (i.e., JPEG, JPEG2K, WN, and Blur) are included, and logistic regression is applied to match the predicted DMOS to MOS value [50, 53].

The results provided in Table 3 demonstrate the generalization ability of our approach. As shown in Table 3, *QualNet* outperforms all existing algorithms in terms of LCC. It also achieves comparable results in terms of SROCC. Although [19] and [35] achieved higher results compared to our method, it worth mentioning that they both use more learning parameters in their models. [19] and [35] used Resnet50 and VGG19 as their backbones, respectively. For the distortion type prediction task, *QualNet* predicted the distortion types of TID2008 images with 92% accuracy while trained on LIVE images.

To validate if our proposed method is consistent with human visual perception, we visualize the feature maps of *conv1_1* and *conv4_3* blocks in Fig. 3. The first row in Fig. 3 shows five different distortion types from TID2013, including Local block-wise distortions of different intensity (first column), JPEG (second column), JPEG2000 (third column), JPEG transmission errors (fourth column), and Gaussian noise (fifth column). The second and third rows correspond to the feature maps of *conv1_1* and *conv4_3* blocks, respectively. In contrast to recent methods that used the reference

Table 2: Comparison of *QualNet* vs. various NR-IQA algorithms on different datasets. Bold entries are the best and second-best performers.

Method	LIVE		CSIQ		TID2013		LIVE-MD1		LIVE-MD2		Average	
	SROCC	LCC	SROCC	LCC	SROCC	LCC	SROCC	LCC	SROCC	LCC	SROCC	LCC
DIIVINE[51]	0.892	0.908	0.804	0.776	0.643	0.567	0.909	0.931	0.831	0.874	0.815	0.811
BRISQUE[41]	0.929	0.944	0.812	0.748	0.626	0.571	0.904	0.936	0.861	0.888	0.826	0.817
NIQE[42]	0.908	0.948	0.812	0.629	0.421	0.330	0.861	0.911	0.782	0.844	0.765	0.732
IL-NIQE[75]	0.902	0.906	0.822	0.865	0.521	0.648	0.881	0.857	0.871	0.869	0.799	0.829
BIECON[25]	0.958	0.961	0.815	0.823	0.717	0.762	-	-	-	-	0.830	0.848
IQA-CNN++ [23]	0.965	0.966	0.892	0.905	0.872	0.878	0.953	0.942	0.943	0.905	0.925	0.919
CNN-SWA[60]	0.982	0.974	0.887	0.891	0.880	0.851	0.934	0.921	0.931	0.921	0.922	0.891
MEON[39]	0.951	0.955	0.852	0.864	0.808	0.824	0.915	0.934	0.953	0.949	0.895	0.905
HFD-BIQA[64]	0.951	0.972	0.842	0.890	0.764	0.681	-	-	-	-	0.852	0.847
WaDIQaM-NR[2]	0.960	0.955	0.852	0.844	0.835	0.855	-	-	-	-	0.882	0.884
BPSQM[44]	0.973	0.963	0.874	0.915	0.862	0.885	0.867	0.898	0.891	0.912	0.893	0.914
Hallucinated-IQA[35]	0.982	0.982	0.885	0.910	0.879	0.880	-	-	-	-	0.915	0.924
DIQA [26]	0.975	0.977	0.884	0.915	0.825	0.850	0.945	0.951	0.932	0.944	0.912	0.927
Ref. [19]	0.970	0.971	0.889	0.894	0.862	0.884	0.927	0.926	0.932	0.939	0.916	0.922
NRVPD[33]	0.956	0.960	0.886	0.918	0.749	0.808	0.937	0.942	0.924	0.941	0.890	0.913
QualNet (proposed)	0.980	0.984	0.907	0.921	0.890	0.901	0.961	0.965	0.960	0.952	0.938	0.943

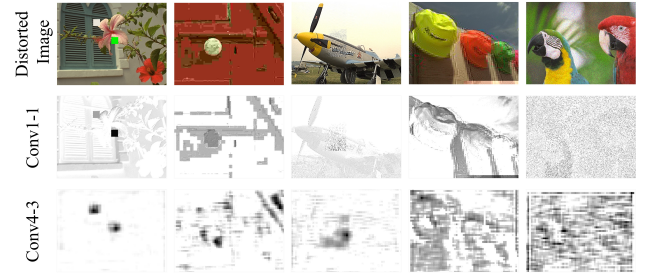
Table 3: SROCC and LCC comparison of various NR-IQA models trained using LIVE dataset and tested on the TID2008 dataset. Bold entries are the best and second-best performers.

Methods	SROCC	LCC
CORNIA [71]	0.880	0.890
CNN [22]	0.920	0.903
SOM [76]	0.923	0.899
IQA-CNN++ [23]	0.917	0.921
CNN-SWA [60]	0.915	0.922
dipIQ [38]	0.916	0.918
MEON [39]	0.921	0.918
WaDIQaM-NR [2]	0.919	0.916
DIQA [26]	0.922	-
BPSQM [44]	0.910	-
HIQA [35]	0.934	0.917
Ref. [19]	0.935	0.936
NRVPD [33]	0.904	0.908
QualNet (Proposed)	0.925	0.940

images to teach their networks to focus on distorted areas and generate a quality map, Fig. 3 shows that our method automatically learns the distortions and highlight them. The dark areas in images in the second and third rows in Fig. 3 indicate distorted regions. We observe that our proposed model learns to focus on the distortions instead of the content of images. For instance, the last row of Fig. 3 clearly shows that for a noisy image our method captures the noise artifacts instead of the image texture/content.

4.3 Screen Content Images

Most of the NR-IQA algorithms were developed for natural images and they do not typically perform well on SCIs. Here we show that

**Figure 3: Illustration of the feature maps of the *conv1_1* block (2nd row) and *conv4_3* block (3rd row) for images with different distortion types. Distorted images (1st row) are taken from TID2013 dataset. From first to fifth column the images have JPEG, JPEG2000, JPEG transmission errors, and Gaussian noise distortions, respectively. The images in the third row are resized for illustration purposes.**

our proposed method not only performs well on natural images, but it also works well for images with other contents.

Unlike natural images, SCIs include diverse forms of visual content, such as pictorial and textual regions. Therefore, the characteristics of SCIs and those of natural images are greatly different. Recently, there have been some metrics that designed specifically for the visual quality prediction of SCIs [9, 13, 15, 63]. Here we use SIQAD dataset to evaluate the performance of *QualNet* on SCIs. The SIQAD dataset includes 980 screen content images corrupted by conventional distortion types (e.g. JPEG, blur, noise, etc). Table 4 provides a comparison between our results and various modern NR-IQA algorithms designed either for natural images [2, 19, 23, 42, 75] or specifically for SCIs [9, 13, 15, 63]. The results show that our algorithm yields a high correlation with the subjective quality ratings and yields the best results in terms of both LCC and SROCC.

Table 4: Comparison of *QualNet* vs. various NR-IQA algorithms on SIQAD dataset. Bold entries are the best and second-best performers.

Database	SIQAD	
Methods	SROCC	LCC
NIQE [42]	0.482	0.500
IL-NIQE [75]	0.517	0.540
IQA-CNN++ [23]	0.702	0.721
CNN-SWA [60]	0.725	0.735
BMS [13]	0.725	0.756
ASIQE [15]	0.757	0.788
NRLT [9]	0.820	0.844
WaDIQaM-NR [2]	0.852	0.859
Ref. [63]	0.811	0.833
Ref. [19]	0.844	0.856
QualNet (Proposed)	0.853	0.862

4.4 HDR-processed images

There is a growing practice of acquiring/creating and displaying high dynamic range (HDR) images and other types of pictures created by multiple exposure fusion. These kinds of images allow for more pleasing representation and better use of the available luminance and color ranges in real scenes, which can range from direct sunlight to faint starlight [48]. HDR images typically are obtained by blending a stack of Standard Dynamic Range (SDR) images at varying exposure levels, HDR images need to be tone-mapped to SDR for display on standard monitors. Multi Exposure Fusion (MEF) techniques are also used to bypass HDR creation by fusing an exposure stack directly to SDR images to achieve aesthetically pleasing luminance and color distributions. HDR images may also be post-processed (color saturation, color temperature, detail enhancement, etc.) for aesthetic purposes. Therefore, due to different types of tone mapping, multi-exposure fusion, and post-processing techniques, HDR images can go under different types of distortions that are different from conventional distortions.

To demonstrate the effectiveness of *QualNet* and its application for NR-IQA in different domains we conduct an experiment where we evaluate the performance of several state-of-the-art NR-IQA algorithms on the recently developed ESPL-LIVE HDR dataset. The images in the ESPL-LIVE HDR dataset were obtained using 11 HDR processing algorithms involving both tone-mapping and MEF. ESPL-LIVE HDR dataset also considered post-processing artifacts of HDR image creation, which typically occur in commercial HDR systems.

Table 5 provides a comparison between our results and various modern NR-IQA algorithms designed either for natural images [2, 19, 23, 51, 60, 67] or specifically for HDR-processed images [3, 12, 21, 30]. The results show that our algorithm outperforms existing algorithms in terms of both SROCC and LCC and yields a high correlation with the subjective quality ratings.

Table 5: Comparison of *QualNet* vs. various NR-IQA algorithms on ESPL-LIVE HDR dataset. Bold entries are the best and second-best performers.

Database	ESPL-LIVE HDR	
Methods	SROCC	LCC
DIIVINE [51]	0.523	0.530
GM-LOG [67]	0.549	0.562
IQA-CNN++ [23]	0.673	0.685
CNN-SWA [60]	0.66	0.672
Ref. [19]	0.701	0.695
BTMQI [12]	0.668	0.673
WaDIQaM-NR [2]	0.752	0.762
BLIQUE-TMI [21]	0.704	0.712
HIGRADE [30]	0.695	0.696
Ref. [3]	0.763	0.768
QualNet (Proposed)	0.796	0.786

4.5 Distortion Prediction

Although the main focus of this paper is on NR-IQA, in Table 6 we provide the results of the distortion type prediction task for our proposed model. As shown in Table 6, *QualNet* achieves good prediction accuracy over different datasets.

Table 6: Performance of our proposed model for distortion type prediction task on different datasets.

datasets	LIVE	CSIQ	TID2008	TID2013
Distortion Prediction (%)	83	93	89	91
datasets	LIVE-MD1	LIVE-MD2	SIQAD	ESPL-LIVE HDR
Distortion Prediction (%)	97	96	98	68

4.6 Ablation Studies

To investigate the effectiveness of our module and training scheme, we provide a comprehensive ablation study in this section. For each ablated model we train it on the subsets of the LIVE dataset and test it on the subsets of TID2013, where four distortion types (i.e., JPEG, JPEG2K, WN, and Blur) are included.

Fig. 4 demonstrates different network architectures for our ablation study. Fig. 4 (a) shows a model with just quality score regression task (single-task) while using fully connected layers for the regression task; Fig. 4 (b) is the same as Fig. 4 (a) while replacing the fully connected layers with 1×1 convolution along with GAP. Fig. 4 (c) shows the model in a multi-task manner, but both quality score and distortion type prediction are done by using the features from the last layer without any feature fusion. Fig. 4 (d) shows the model in a multi-task manner, while the quality score and distortion prediction are done by using the features from different layers in the network without any feature fusion. Fig. 4 (e) shows the model in a multi-task manner, while feature fusion is performed from the last layer for quality estimation. Fig. 4 (f) is our proposed method.

Table 7 shows the results of different ablated models from Fig. 4. As we can see model-a and model-b achieve the lowest performance

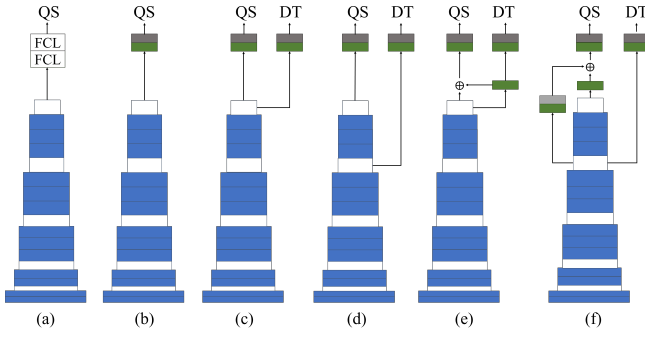


Figure 4: Exploring different network architectures for NR-IQA task. QS and DT stand for quality score and distortion type, respectively. (a) and (b) show single-task models, where they are using FCL and 1×1 convolution along with GAP, respectively, in the last layer for quality score estimation. (c)-(f) show a multi-task model while having different architectures.

comparing to the multi-task models. This proves our hypothesis that using distortion type knowledge along with quality score can improve the results. Moreover, we observe that model-b outperforms model-a; in our experiments, we observe that using fully connected layers while having limited training data will cause the model to overfit to the training data quickly which causes a lack of generality in the test phase. Furthermore, as shown in Table 7, both model-c and model-d achieve very similar results, but worse than model-f. This demonstrates the effectiveness of our feature fusion method. Finally, we observe that using the features from different layers for each task leads to better performance. In Table 7 we also provide the performance evaluation of our model via SGD for optimization. We observe that using SGD can cause the network to converge slower and lead to slightly worse results. Finally we provide results of our model while using different patch sizes as an input. We can see that while patch size of 128 leads to the best results as we move to 64 and 32 the performance degrades more. The main reason for dropping the performance while using smaller patch sizes is that the small patches do not have enough content information to represent the ground truth subjective score of the distorted image. In this paper, we select VGG16 as our backbone to show the effectiveness of our model to other methods that chose deeper backbones. However, as shown in Table 7 (Model-f-VGG-19) using a deeper network (e.g. VGG19) can improve our results even more.

5 CONCLUSION

In this paper, we proposed a simple yet effective multi-task model, *QualNet*, for general-purpose no-reference image quality assessment (NR-IQA). Our model exploits distortion type as well as subjective human scores. We demonstrate that by employing multi-task learning as well as our proposed feature fusion method, our model achieves better performance across different datasets. Our experimental results show that the proposed model achieves high accuracy while maintaining consistency with human perceptual quality assessments.

Table 7: Ablation study results

Methods	Optimization	Patch Size	SROCC	LCC
Model-a	ADAM	128×128	0.862	0.882
Model-b	ADAM	128×128	0.870	0.902
Model-c	ADAM	128×128	0.905	0.918
Model-d	ADAM	128×128	0.902	0.922
Model-e	ADAM	128×128	0.906	0.920
Model-f (Proposed)	ADAM	128×128	0.916	0.936
Model-f-V2	SGD	128×128	0.909	0.929
Model-f-V3	ADAM	64×64	0.891	0.911
Model-f-V4	ADAM	32×32	0.878	0.889
Model-f-VGG-19	ADAM	128×128	0.925	0.945

REFERENCES

- [1] Md Mushfiqul Alam, Kedarnath P Vilankar, David J Field, and Damon M Chandler. 2014. Local masking in natural images: A database and analysis. *Journal of vision* 14, 8 (2014), 22–22.
- [2] Sebastian Bosse, Dominique Maniry, Klaus-Robert Müller, Thomas Wiegand, and Wojciech Samek. 2017. Deep neural networks for no-reference and full-reference image quality assessment. *IEEE Transactions on Image Processing* 27, 1 (2017), 206–219.
- [3] Pengfei Chen, Leida Li, Xinfeng Zhang, Shanshe Wang, and Allen Tan. 2019. Blind quality index for tone-mapped images based on luminance partition. *Pattern Recognition* 89 (2019), 108–118.
- [4] Chun-Hsien Chou and Yun-Chin Li. 1995. A perceptually tuned subband image coder based on the measure of just-noticeable-distortion profile. *IEEE Transactions on circuits and systems for video technology* 5, 6 (1995), 467–476.
- [5] Scott J Daly. 1992. Visible differences predictor: an algorithm for the assessment of image fidelity. In *Human Vision, Visual Processing, and Digital Display III*, Vol. 1666. International Society for Optics and Photonics, 2–15.
- [6] Jia Deng, Wei Dong, Richard Socher, Li-Jia Li, Kai Li, and Li Fei-Fei. 2009. Imagenet: A large-scale hierarchical image database. In *2009 IEEE conference on computer vision and pattern recognition*. Ieee, 248–255.
- [7] Samuel Dodge and Lina Karam. 2016. Understanding how image quality affects deep neural networks. In *2016 eighth international conference on quality of multimedia experience (QoMEX)*. IEEE, 1–6.
- [8] David Eigen and Rob Fergus. 2015. Predicting depth, surface normals and semantic labels with a common multi-scale convolutional architecture. In *Proceedings of the IEEE international conference on computer vision*. 2650–2658.
- [9] Yuming Fang, Jiebin Yan, Leida Li, Jinjian Wu, and Weisi Lin. 2017. No reference quality assessment for screen content images with both local and global feature representation. *IEEE Transactions on Image Processing* 27, 4 (2017), 1600–1610.
- [10] Deepti Ghadiyaram and Alan C Bovik. 2017. Perceptual quality prediction on authentically distorted images using a bag of features approach. *Journal of vision* 17, 1 (2017), 32–32.
- [11] SeyedAlireza Golestaneh and Lina J Karam. 2016. Reduced-reference quality assessment based on the entropy of DWT coefficients of locally weighted gradient magnitudes. *IEEE Transactions on Image Processing* 25, 11 (2016), 5293–5303.
- [12] Ke Gu, Shiqi Wang, Guangtao Zhai, Siwei Ma, Xiaokang Yang, Weisi Lin, Wenjun Zhang, and Wen Gao. 2016. Blind quality assessment of tone-mapped images via analysis of information, naturalness, and structure. *IEEE Transactions on Multimedia* 18, 3 (2016), 432–443.
- [13] Ke Gu, Guangtao Zhai, Weisi Lin, Xiaokang Yang, and Wenjun Zhang. 2016. Learning a blind quality evaluation engine of screen content images. *Neurocomputing* 196 (2016), 140–149.
- [14] Ke Gu, Guangtao Zhai, Xiaokang Yang, and Wenjun Zhang. 2014. Using free energy principle for blind image quality assessment. *IEEE Transactions on Multimedia* 17, 1 (2014), 50–63.
- [15] Ke Gu, Jun Zhou, Jun-Fei Qiao, Guangtao Zhai, Weisi Lin, and Alan Conrad Bovik. 2017. No-reference quality assessment of screen content pictures. *IEEE Transactions on Image Processing* 26, 8 (2017), 4005–4018.
- [16] Jun Guo and Hongyang Chao. 2017. Building an end-to-end spatial-temporal convolutional network for video super-resolution. In *Thirty-First AAAI Conference on Artificial Intelligence*.
- [17] Kaiming He, Xiangyu Zhang, Shaoqing Ren, and Jian Sun. 2016. Deep residual learning for image recognition. In *Proceedings of the IEEE conference on computer vision and pattern recognition*. 770–778.
- [18] Lihuo He, Dacheng Tao, Xuelong Li, and Xinbo Gao. 2012. Sparse representation for blind image quality assessment. In *2012 IEEE Conference on Computer Vision and Pattern Recognition*. IEEE, 1146–1153.

- [19] Yuge Huang, Xiang Tian, Yaowu Chen, and Rongxin Jiang. 2018. Multitask convolutional neural network for no-reference image quality assessment. *Journal of Electronic Imaging* 27, 6 (2018), 063033.
- [20] Dinesh Jayaraman, Anish Mittal, Anush K Moorthy, and Alan C Bovik. 2012. Objective quality assessment of multiply distorted images. In *2012 Conference record of the forty sixth asilomar conference on signals, systems and computers (ASILOMAR)*. IEEE, 1693–1697.
- [21] Qiuping Jiang, Feng Shao, Weisi Lin, and Gangyi Jiang. 2017. BLIQUE-TMI: Blind quality evaluator for tone-mapped images based on local and global feature analyses. *IEEE Transactions on Circuits and Systems for Video Technology* 29, 2 (2017), 323–335.
- [22] Le Kang, Peng Ye, Yi Li, and David Doermann. 2014. Convolutional neural networks for no-reference image quality assessment. In *Proceedings of the IEEE conference on computer vision and pattern recognition*. 1733–1740.
- [23] Le Kang, Peng Ye, Yi Li, and David Doermann. 2015. Simultaneous estimation of image quality and distortion via multi-task convolutional neural networks. In *2015 IEEE international conference on image processing (ICIP)*. IEEE, 2791–2795.
- [24] Jongyoo Kim and Sanghoon Lee. 2017. Deep learning of human visual sensitivity in image quality assessment framework. In *Proceedings of the IEEE conference on computer vision and pattern recognition*. 1676–1684.
- [25] Jongyoo Kim and Sanghoon Lee. 2017. Fully Deep Blind Image Quality Predictor. *IEEE Journal on Selected Topics in Signal Processing* 11, 1 (2017), 206–220.
- [26] Jongyoo Kim, Anh-Duc Nguyen, and Sanghoon Lee. 2018. Deep CNN-based blind image quality predictor. *IEEE transactions on neural networks and learning systems* 30, 1 (2018), 11–24.
- [27] Diederik P Kingma and Jimmy Ba. 2014. Adam: A method for stochastic optimization. *arXiv preprint arXiv:1412.6980* (2014).
- [28] Alex Krizhevsky, Ilya Sutskever, and Geoffrey E Hinton. 2012. Imagenet classification with deep convolutional neural networks. In *Advances in neural information processing systems*. 1097–1105.
- [29] Debarati Kundu, Deepti Ghadiyaram, Alan C Bovik, and Brian L Evans. 2017. Large-scale crowdsourced study for tone-mapped HDR pictures. *IEEE Transactions on Image Processing* 26, 10 (2017), 4725–4740.
- [30] Debarati Kundu, Deepti Ghadiyaram, Alan C Bovik, and Brian L Evans. 2017. No-reference quality assessment of tone-mapped HDR pictures. *IEEE Transactions on Image Processing* 26, 6 (2017), 2957–2971.
- [31] Eric Cooper Larson and Damon Michael Chandler. 2010. Most apparent distortion: full-reference image quality assessment and the role of strategy. *Journal of Electronic Imaging* 19, 1 (2010), 011006.
- [32] Gordon E Legge and John M Foley. 1980. Contrast masking in human vision. *Josa* 70, 12 (1980), 1458–1471.
- [33] Qiaohong Li, Weisi Lin, Ke Gu, Yabin Zhang, and Yuming Fang. 2019. Blind image quality assessment based on joint log-contrast statistics. *Neurocomputing* 331 (2019), 189–198.
- [34] Yudong Liang, Jinjun Wang, Xingyu Wan, Yihong Gong, and Nanning Zheng. 2016. Image quality assessment using similar scene as reference. In *European Conference on Computer Vision*. Springer, 3–18.
- [35] Kwan-Yee Lin and Guanxiang Wang. 2018. Hallucinated-IQA: No-reference image quality assessment via adversarial learning. In *Proceedings of the IEEE Conference on Computer Vision and Pattern Recognition*. 732–741.
- [36] Xialei Liu, Joost van de Weijer, and Andrew D Bagdanov. 2017. Rankiq: Learning from rankings for no-reference image quality assessment. In *Proceedings of the IEEE International Conference on Computer Vision*. 1040–1049.
- [37] Yu Liu, Junjie Yan, and Wanli Ouyang. 2017. Quality aware network for set to set recognition. In *Proceedings of the IEEE Conference on Computer Vision and Pattern Recognition*. 5790–5799.
- [38] Kede Ma, Wentao Liu, Tongliang Liu, Zhou Wang, and Dacheng Tao. 2017. dipIQ: Blind image quality assessment by learning-to-rank discriminable image pairs. *IEEE Transactions on Image Processing* 26, 8 (2017), 3951–3964.
- [39] Kede Ma, Wentao Liu, Kai Zhang, Zhengfang Duanmu, Zhou Wang, and Wang-meng Zuo. 2017. End-to-end blind image quality assessment using deep neural networks. *IEEE Transactions on Image Processing* 27, 3 (2017), 1202–1213.
- [40] Xiongkui Min, Ke Gu, Guangtao Zhai, Jing Liu, Xiaokang Yang, and Chang Wen Chen. 2017. Blind quality assessment based on pseudo-reference image. *IEEE Transactions on Multimedia* 20, 8 (2017), 2049–2062.
- [41] Anish Mittal, Anush Krishna Moorthy, and Alan Conrad Bovik. 2012. No-reference image quality assessment in the spatial domain. *IEEE Transactions on image processing* 21, 12 (2012), 4695–4708.
- [42] Anish Mittal, Rajiv Soundararajan, and Alan C Bovik. 2012. Making a completely blind image quality analyzer. *IEEE Signal Processing Letters* 20, 3 (2012), 209–212.
- [43] Anush Krishna Moorthy and Alan Conrad Bovik. 2011. Blind image quality assessment: From natural scene statistics to perceptual quality. *IEEE transactions on Image Processing* 20, 12 (2011), 3350–3364.
- [44] Da Pan, Ping Shi, Ming Hou, Zefeng Ying, Sizhe Fu, and Yuan Zhang. 2018. Blind predicting similar quality map for image quality assessment. In *Proceedings of the IEEE Conference on Computer Vision and Pattern Recognition*. 6373–6382.
- [45] Xingchao Peng, Baochen Sun, Karim Ali, and Kate Saenko. 2015. Learning deep object detectors from 3d models. In *Proceedings of the IEEE International Conference on Computer Vision*. 1278–1286.
- [46] Nikolay Ponomarenko, Oleg Ieremeiev, Vladimir Lukin, Karen Egiazarian, Lina Jin, Jaakko Astola, Benoit Vozel, Kacem Chehdi, Marco Carli, Federica Battisti, et al. 2013. Color image database TID2013: Peculiarities and preliminary results. In *European workshop on visual information processing (EUVIP)*. IEEE, 106–111.
- [47] Nikolay Ponomarenko, Vladimir Lukin, Alexander Zelensky, Karen Egiazarian, Marco Carli, and Federica Battisti. 2009. TID2008-a database for evaluation of full-reference visual quality assessment metrics. *Advances of Modern Radioelectronics* 10, 4 (2009), 30–45.
- [48] Erik Reinhard, Wolfgang Heidrich, Paul Debevec, Sumanta Pattanaik, Greg Ward, and Karol Myszkowski. 2010. *High dynamic range imaging: acquisition, display, and image-based lighting*. Morgan Kaufmann.
- [49] Zhongzheng Ren and Yong Jae Lee. 2018. Cross-domain self-supervised multi-task feature learning using synthetic imagery. In *Proceedings of the IEEE Conference on Computer Vision and Pattern Recognition*. 762–771.
- [50] Ann Marie Rohaly, Philip J Coriveau, John M Libert, Arthur A Webster, Vittorio Baroncini, John Beerends, Jean-Louis Blin, Laura Contin, Takahiro Hamada, David Harrison, et al. 2000. Video quality experts group: Current results and future directions. In *Visual Communications and Image Processing 2000*, Vol. 4067. International Society for Optics and Photonics, 742–753.
- [51] Michele A Saad, Alan C Bovik, and Christophe Charrier. 2012. Blind image quality assessment: A natural scene statistics approach in the DCT domain. *IEEE transactions on Image Processing* 21, 8 (2012), 3339–3352.
- [52] Hamid R Sheikh, Alan C Bovik, and Gustavo De Veciana. 2005. An information fidelity criterion for image quality assessment using natural scene statistics. *IEEE Transactions on image processing* 14, 12 (2005), 2117–2128.
- [53] Hamid R Sheikh, Muhammad F Sabir, and Alan C Bovik. 2006. A statistical evaluation of recent full reference image quality assessment algorithms. *IEEE Transactions on image processing* 15, 11 (2006), 3440–3451.
- [54] Karen Simonyan and Andrew Zisserman. 2014. Very deep convolutional networks for large-scale image recognition. *arXiv preprint arXiv:1409.1556* (2014).
- [55] Rajiv Soundararajan and Alan C Bovik. 2011. RRED indices: Reduced reference entropic differencing for image quality assessment. *IEEE Transactions on Image Processing* 21, 2 (2011), 517–526.
- [56] Christian Szegedy, Wei Liu, Yangqing Jia, Pierre Sermanet, Scott Reed, Dragomir Anguelov, Dumitru Erhan, Vincent Vanhoucke, and Andrew Rabinovich. 2015. Going deeper with convolutions. In *Proceedings of the IEEE conference on computer vision and pattern recognition*. 1–9.
- [57] Hossein Talebi and Peyman Milanfar. 2018. Nima: Neural image assessment. *IEEE Transactions on Image Processing* 27, 8 (2018), 3998–4011.
- [58] Huixuan Tang, Neel Joshi, and Ashish Kapoor. 2011. Learning a blind measure of perceptual image quality. In *CVPR 2011*. IEEE, 305–312.
- [59] Huixuan Tang, Neel Joshi, and Ashish Kapoor. 2014. Blind image quality assessment using semi-supervised rectifier networks. In *Proceedings of the IEEE Conference on Computer Vision and Pattern Recognition*. 2877–2884.
- [60] Hanli Wang, Lingxuan Zuo, and Jie Fu. 2016. Distortion recognition for image quality assessment with convolutional neural network. In *2016 IEEE International Conference on Multimedia and Expo (ICME)*. IEEE, 1–6.
- [61] Zhou Wang and Alan C Bovik. 2006. Modern image quality assessment. *Synthesis Lectures on Image, Video, and Multimedia Processing* 2, 1 (2006), 1–156.
- [62] Andrew B Watson and Albert J Ahumada. 2005. A standard model for foveal detection of spatial contrast. *Journal of vision* 5, 9 (2005), 6–6.
- [63] Jun Wu, Zhaoqiang Xia, Huiqing Zhang, and Huifang Li. 2019. Blind quality assessment for screen content images by combining local and global features. *Digital Signal Processing* 91 (2019), 31–40.
- [64] Jinjian Wu, Jichen Zeng, Yongxu Liu, Guangming Shi, and Weisi Lin. 2017. Hierarchical feature degradation based blind image quality assessment. In *Proceedings of the IEEE International Conference on Computer Vision*. 510–517.
- [65] Qingbo Wu, Hongliang Li, King N Ngan, Bing Zeng, and Moncef Gabbouj. 2014. No reference image quality metric via distortion identification and multi-channel label transfer. In *2014 IEEE International Symposium on Circuits and Systems (ISCAS)*. IEEE, 530–533.
- [66] Long Xu, Jia Li, Weisi Lin, Yongbing Zhang, Lin Ma, Yuming Fang, and Yihua Yan. 2016. Multi-task rank learning for image quality assessment. *IEEE Transactions on Circuits and Systems for Video Technology* 27, 9 (2016), 1833–1843.
- [67] Wufeng Xue, Xuanqin Mou, Lei Zhang, Alan C Bovik, and Xiangchu Feng. 2014. Blind image quality assessment using joint statistics of gradient magnitude and Laplacian features. *IEEE Transactions on Image Processing* 23, 11 (2014), 4850–4862.
- [68] Wufeng Xue, Lei Zhang, and Xuanqin Mou. 2013. Learning without human scores for blind image quality assessment. In *Proceedings of the IEEE Conference on Computer Vision and Pattern Recognition*. 995–1002.
- [69] Huan Yang, Yuming Fang, and Weisi Lin. 2015. Perceptual quality assessment of screen content images. *IEEE Transactions on Image Processing* 24, 11 (2015), 4408–4421.

- [70] Peng Ye, Jayant Kumar, and David Doermann. 2014. Beyond human opinion scores: Blind image quality assessment based on synthetic scores. In *Proceedings of the IEEE Conference on Computer Vision and Pattern Recognition*. 4241–4248.
- [71] Peng Ye, Jayant Kumar, Le Kang, and David Doermann. 2012. Unsupervised feature learning framework for no-reference image quality assessment. In *2012 IEEE conference on computer vision and pattern recognition*. IEEE, 1098–1105.
- [72] Zhenqiang Ying, Haoran Niu, Praful Gupta, Dhruv Mahajan, Deepti Ghadiyaram, and Alan Bovik. 2020. From Patches to Pictures (PaQ-2-PiQ): Mapping the Perceptual Space of Picture Quality. (2020).
- [73] Guanghui Yue, Chunping Hou, Ke Gu, Nam Ling, and Beichen Li. 2018. Analysis of structural characteristics for quality assessment of multiply distorted images. *IEEE Transactions on Multimedia* 20, 10 (2018), 2722–2732.
- [74] Kai Zhang, Wangmeng Zuo, Shuhang Gu, and Lei Zhang. 2017. Learning deep CNN denoiser prior for image restoration. In *Proceedings of the IEEE conference on computer vision and pattern recognition*. 3929–3938.
- [75] Lin Zhang, Lei Zhang, and Alan C Bovik. 2015. A feature-enriched completely blind image quality evaluator. *IEEE Transactions on Image Processing* 24, 8 (2015), 2579–2591.
- [76] Peng Zhang, Wengang Zhou, Lei Wu, and Houqiang Li. 2015. SOM: Semantic obviousness metric for image quality assessment. In *Proceedings of the IEEE Conference on Computer Vision and Pattern Recognition*. 2394–2402.
- [77] Richard Zhang, Phillip Isola, Alexei A Efros, Eli Shechtman, and Oliver Wang. 2018. The unreasonable effectiveness of deep features as a perceptual metric. In *Proceedings of the IEEE Conference on Computer Vision and Pattern Recognition*. 586–595.
- [78] Yi Zhang and Damon M Chandler. 2018. Opinion-unaware blind quality assessment of multiply and singly distorted images via distortion parameter estimation. *IEEE Transactions on Image Processing* 27, 11 (2018), 5433–5448.
- [79] Yuke Zhu, Roozbeh Mottaghi, Eric Kolve, Joseph J Lim, Abhinav Gupta, Li Fei-Fei, and Ali Farhadi. 2017. Target-driven visual navigation in indoor scenes using deep reinforcement learning. In *2017 IEEE international conference on robotics and automation (ICRA)*. IEEE, 3357–3364.